Studies on Optimal Application of Building-Integrated Photovoltaic/Thermal Facade for Commercial Buildings in Australia

Siliang Yang[1], Francesco Fiorito[2], Alistair Sproul[3] and Deo Prasad[4]

[1] Faculty of the Built Environment, UNSW, Sydney NSW 2052, Australia

[2] Department of Civil, Environmental, Land, Building Engineering and Chemistry, Polytechnic University of Bari, 70125 Bari, Italy

[3] School of Photovoltaic & Renewable Energy Engineering, UNSW, Sydney NSW 2052, Australia

[4] Cooperative Research Centre for Low Carbon Living (CRC-LCL), Sydney NSW 2052, Australia

Abstract

Both electrical power and useful thermal energy can be obtained from building-integrated photovoltaic/thermal systems (BIPV/T) which have the potential to reduce the energy consumption of buildings. Double-skin façades (DSF) have been implemented for enhancing energy efficiency as well as improving indoor thermal comfort. This paper explored the performance of a combination of BIPV/T and DSF, which included the thermal performance of this novel building envelope as well as the indoor comfort performance through a simulation analysis for a test building in Sydney, Australia. To date, the work has focused on two operation modes of the BIPV/T-DSF system comprising fan-driven ventilation mode in summer time and non-ventilation mode in winter. A comparative simulation analysis of the two operation modes and the building without adopting the BIPV/T-DSF system was presented in terms of the thermal response of the indoor space.

Keywords: Building-integrated Photovoltaic/Thermal System, Double-skin Façade, Commercial Building, Energy Efficiency, Indoor Thermal Comfort

1. Introduction

The world is in the process of rapid development, with increasing heavy industrial production as well as increasing building construction, all of which is contributing to the rapid increase of energy consumption. Energy demand from the building sector accounts for 40% of energy consumption globally and consequently emits approximately 1/3 of the greenhouse gas emissions (United Nations Environment Programme, 2016). The total energy consumption of commercial buildings in Australia was 3.5% of the national gross energy consumption in 2009 and this proportion is expected to rise by 24% over the period 2009 to 2020 (Council of Australian Governments, 2012). Building façades are a key component linking buildings and the outdoor environment, which significantly affects air-conditioning energy use for heating and cooling (Peng, Lu, Yang, Song, & Ma, 2015). High heating and cooling energy consumption is due to the poor thermal insulation properties of building façade (Papaefthimiou, Syrrakou, & Yianoulis, 2006). Thus, exploring high performance building façades is important to improve energy efficiency of commercial buildings.

The utilization of renewable energy technologies in buildings is an effective solution to combat the increase in energy consumption (Chwieduk, 2017). Solar energy is one of the most widely applied renewable energy approaches for increasing energy sustainability in the building industry (Mekhilef, Saidur, & Safari, 2011). Solar photovoltaic/thermal (PV/T) systems, integrated into building façade, can form a cohesive design, construction and energy solution for buildings (M. D. Bazilian, Leenders, Ree, & Prasad, 2001). Both electrical power and useful thermal energy can be obtained from the PV/T system hence contributing to the reduction of

[1] Corresponding author. Tel.: +61 (02) 9385 6372; Mob.: +61 (0) 415 680 589.
E-mail address: siliang.yang@unsw.edu.au

doi:10.18086/swc.2017.12.13 Available at http://proceedings.ises.org

the energy consumption of a building (Yang & Athienitis, 2012). Double skin façades, have been effective for enhancing energy efficiency as well as improving the indoor thermal comfort (Marques da Silva, Gomes, & Rodrigues, 2015). This type of façade solution has become a globally widespread option for implementing sustainable energy and an architecturally attractive option for the building envelope (Ghaffarianhoseini et al., 2016). Quite a few researchers have generally reported the factors of that affecting the power efficiency of the BIPV system (e.g. typology of the materials, PV module temperature, and packing factor of PV module) (M. Bazilian, Kamalanathan, & Prasad, 2002; Oliver & Jackson, 2000; Vats, Tomar, & Tiwari, 2012). A few studies have reported both the thermal and electrical efficiency of the BIPV/T system but, the outcomes in cold climates have predominated and only a small number investigated a range of climatic conditions (Athienitis, Bambara, O'Neill, & Faille, 2011; Chen, Athienitis, & Galal, 2010; Chow, Hand, & Strachan, 2003; Pantic, Candanedo, & Athienitis, 2010; Yang & Athienitis, 2015). Further a few studies lately reported the performance of PV efficiency of a BIPV/T-DSF envelope, but little research has been done on understanding of indoor thermal comfort and energy performance of the building adopting BIPV/T-DSF system (Charron & Athienitis, 2006; Peng, Lu, & Yang, 2013; Saadon, Gaillard, Giroux-Julien, & Ménézo, 2016). Most of field studies were conducted under the indoor test conditions, which were not absolutely reliable (Fossa, Ménézo, & Leonardi, 2008; Yang & Athienitis, 2015).

Neither building-integrated photovoltaic/thermal (BIPV/T) nor double-skin façade (DSF) is novel. However, little research or real application of the hybrid mechanism of BIPV/T and DSF has been conducted in both academic and industrial settings (Peng, Lu, Yang, & Han, 2013). Therefore, this research project aims to investigate the overall performance of a BIPV/T system integrated with a DSF. In particular the electrical and thermal performance of this novel building envelope as well as the impact of this envelope solution on indoor thermal comfort performance of the commercial buildings is investigated.

2. Methodology

This paper examined both experimental field measurements and computational simulation for building-integrated photovoltaic/thermal double-skin façade (BIPV/T-DSF). The computational model was validated against experimental results reported in the literature. This model was then used to simulate a commercial building in Australia. The system parameters were adjusted to optimize the performance of the BIPV/T-DSF and the indoor thermal condition of the building. A long-term system performance and indoor thermal comfort then can be predicted confidently by using the validated computational model.

The building with BIPV/T-DSF system was modelled in TRNSYS (thermal modelling software). TRNSYS is widely used visual based software for transient simulations of solar thermal energy systems and any dynamic simulation including buildings (Kamel & Fung, 2014).

A model of the BIPV/T-DSF was developed in TRNSYS and validated by using experimental results taken from the existing published studies by Peng et al. (Peng et al., 2016; Peng, Lu, & Yang, 2013; Peng, Lu, Yang, & Ma, 2015). They have conducted the series field studies of a test bed with a ventilated BIPV/T-DSF under different ventilation modes in Hong Kong. This BIPV/T-DSF system uses a double-glazed semi-transparent a-Si PV module (Peng, Lu, & Yang, 2013). The diagram of the BIPV/T-DSF is shown in Fig. 1. As can be seen, the DSF consisted of two cavities which were separated by a vertical insulation board; at this point, the two air cavities were used for the comparative analysis for different modes of ventilation without affecting one another. Two ventilation modes used for model simulation and model validation, are shown in Tab. 1.

Tab. 1: Specifications of the selected ventilation modes for model validation (Peng, Lu, & Yang, 2013).

Ventilation Modes	Specifications
Non-ventilated mode (mode 1)	All inlet and outlet louvers were closed and the internal windows were opened, air-conditioner was turned off.
Buoyancy-driven ventilation mode (mode 2)	The inlet and outlet louvers on left hand side (cavity 1) were closed, while the inlet and outlet louvers on right hand side (cavity 2) were opened; all internal windows were closed; indoor air temperature was maintained at 22°C by use of the air-conditioner.

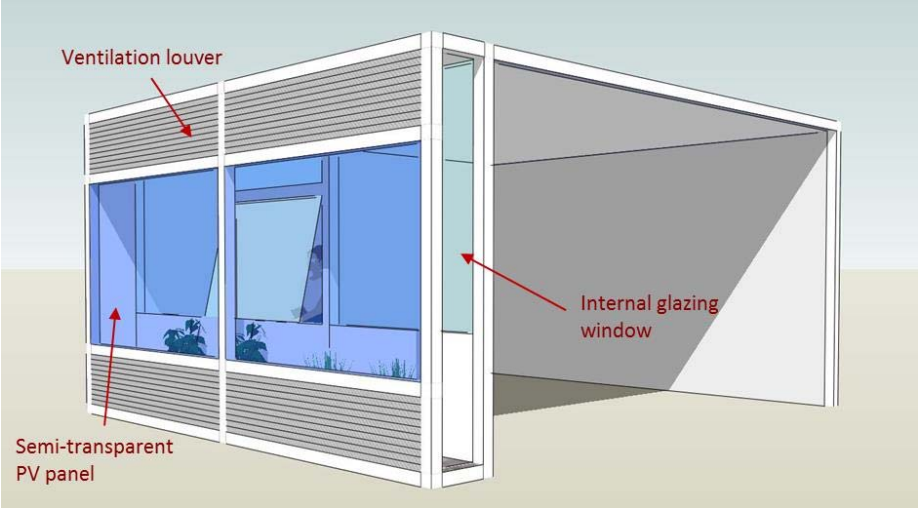

Fig. 1: Schematic diagram of the BIPV/T-DSF system for the test bed (Peng et al., 2016).

3. Modelling and Model Validation

The key dimensions of the BIPV/T-DSF system and the physical characteristics of the PV panel (semi-transparent) used are given in Tab. 2 and Tab. 3 respectively.

Tab. 2: Key dimensions of the BIPV/T-DSF system (Peng et al., 2016).

Parameters	Values
Width of PV panel	1.1 m
Height of PV panel	1.3 m
Thickness of PV module	0.006 m
Width of louver	1.1 m
Height of louver	0.5 m
Depth of air flow duct (air cavity)	0.4 m
Dimension of the test bed (W x L xD)	2.4 x 2.5 x 2.3 m
Orientation	Due south

Tab. 3: Physical characteristics of the semi-transparent a-Si PV panel (Peng et al., 2016).

Parameters	Values
Maximum power under STC (W_p)	85
Open circuit voltage, V_{oc} (V)	134.4
Short circuit current, I_{sc} (A)	1.05
Voltage at the maximum power point, V_{mp} (V)	100
Current at the maximum power point, I_{mp} (A)	0.85
Efficiency, η (%)	6.2
Power temperature coefficient, T_k (%/K)	-0.21
Dimensions (L x W x D), (mm)	1300 x 1100 x 6
Transmittance in visible lighting range (%)	7
Thermal conductivity, ($Wm^{-1}K^{-1}$)	0.486
Infrared emittance	0.85

The test model was established in TRNSYS based on the experimental parameters provided in Tab. 2 and Tab. 3. Real-time meteorological data (on-site historical weather data for Hong Kong) of the site during the experiment was provided by the authors (Peng et al.), which was used for the TRNSYS simulation. Fig. 2 shows the model of the BIPV/T-DSF in the TRNSYS Simulation Studio (the user interface to create the simulation model).

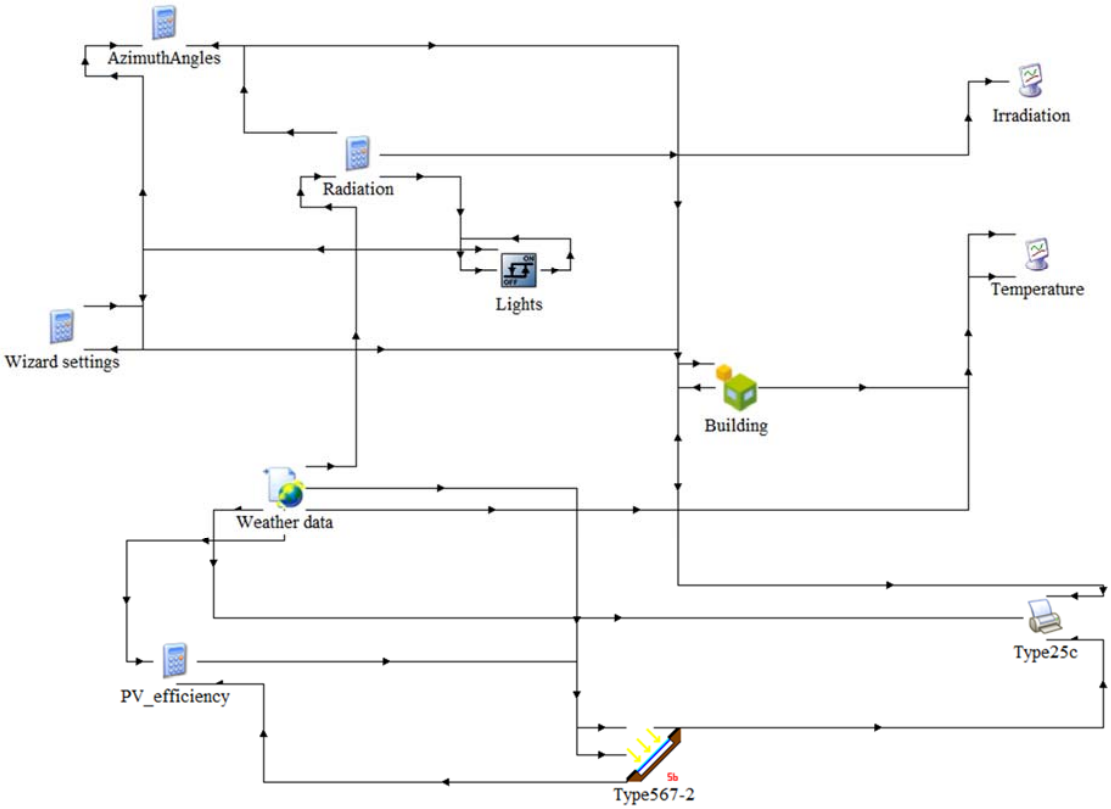

Fig. 2: Schematic of the testing building model integrated with the BIPV/T-DSF system in TRNSYS.

Type 56 (the "building" icon in Fig. 2) included the details of the building model such as building geometry, type of construction, and optical data of the window glazing. The glazed semi-transparent PV panel used in the test bed was symbolized by Type 567-2 (the corresponding PV module in TRNSYS) which was connected to the test bed (Type 56) in the TRNSYS model. Because the semi-transparent PV panel model is not available in TRNSYS, a glazing model with the exact identical thermal and optical properties of the semi-transparent a-Si PV panel was created and replaced the outer window on the DSF. As such, the electricity production of the PV was calculated separately.

3.1. Validation of the Model in Non-Ventilated Mode

The PV module (back-surface) temperature is a major feature that is closely related to the output power of the PV panel, which is mainly affected by the ambient conditions, primarily the solar radiation as well as the ambient temperature (Chikate & Sadawarte, 2015). Therefore, the PV module temperature of the BIPV/T-DSF system from the simulation was compared with the experimental result (Peng, Lu, & Yang, 2013). In addition, the indoor air temperature is a crucial indicator for indoor thermal comfort which was also compared accordingly. The available experimental results of the non-ventilated mode (mode 1) were from Jan 5 to Jan 7, 2013. The simulation in the TRNSYS model was in accordance with the same time period and the comparative results are shown in Fig. 3 and Fig. 4 accordingly.

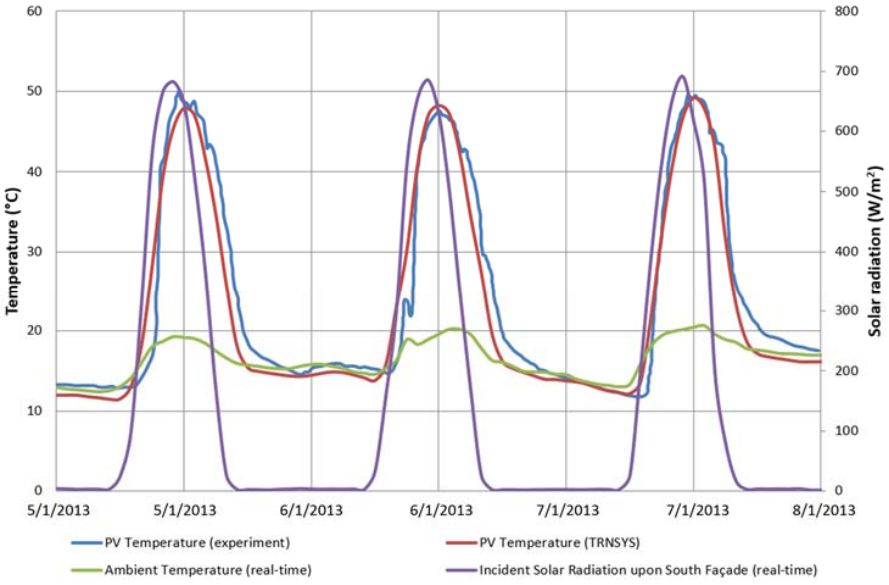

Fig. 3: PV module temperature comparison in Mode 1 (non-ventilated).

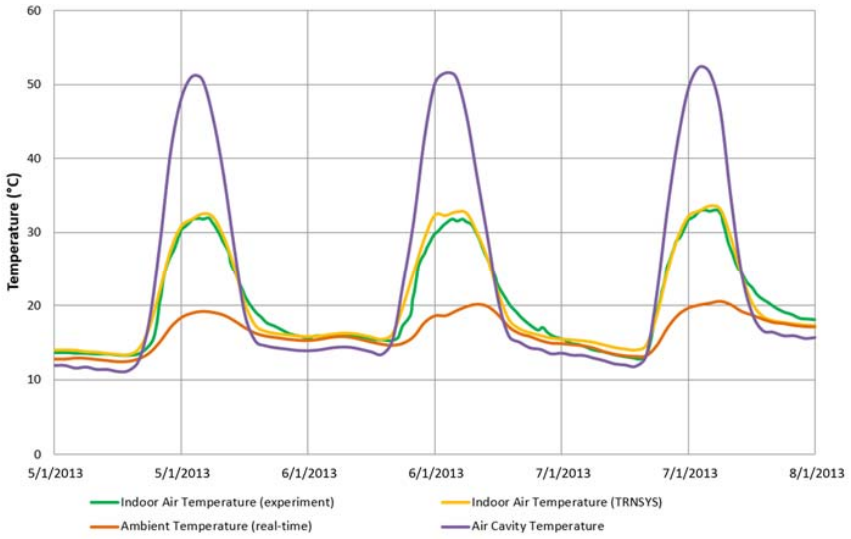

Fig. 4: Indoor air temperature comparison in Mode 1 (non-ventilated).

As can be observed in Fig. 3, the simulated PV module temperature and the measured PV module temperature (72 hours' results) show good agreement although a certain extent of discrepancy exists. The hourly Mean Bias Error (MBE) and Cumulative Variation of Root Mean Squared Error (CVRMSE) (ASHRAE, 2002) were used as the criteria for assessing the acceptability of the agreement between simulated and measured data. The MBE and CVRMSE are calculated as:

$$\boldsymbol{MBE} = \frac{\sum_{i=1}^{Np}(M_i - S_i)}{\sum_{i=1}^{N_P} M_i} \qquad \text{(eq. 1)}$$

$$\overline{\boldsymbol{M_P}} = \frac{\sum_{i=1}^{N_P} M_i}{N_P} \qquad \text{(eq. 2)}$$

$$\boldsymbol{CVRMSE_{(P)}} = \frac{\sqrt{\sum_{i=1}^{N_P}((M_i - S_i)^2 / N_P)}}{\overline{M_P}} \qquad \text{(eq. 3)}$$

Where M_i and S_i are measured and simulated data at instance "i" respectively; p is the interval (e.g. monthly, weekly, daily and hourly); N_p is the number of values at interval p (e.g. $N_{month} = 12$, $N_{day} = 365$, $N_{hour} = 8760$) and $\overline{M_p}$ is the average of the measured data (Raftery, Keane, & Costa, 2011). The both hourly acceptance

thresholds of MBE and CVRMSE are ±10% and ≤30% respectively. For the PV module temperature, the MBE and CVRMSE were 4.55% and 14.48% respectively, so the simulated results of PV module temperature were acceptable. Similarly, as shown in Fig. 4, the hourly values of indoor air temperature also show good agreement with the experimental results and the corresponding hourly MBE and CVRMSE were -1.02% and 5.5% respectively. Thus, the TRNSYS model for mode 1 was deemed validated.

3.2. Validation of the Model in Buoyancy-Driven Ventilation Mode

The available experimental results for the buoyancy-driven ventilation mode were from Jan 28 to Jan 31, 2013. The right-hand side cavity (cavity 2) was selected. As the indoor condition was constantly maintained at 22°C through air-conditioning, the indoor air temperature in this operation mode was not be analyzed. The PV module back surface temperature on this cavity (PV module 2) and internal surface temperature of the corresponding internal window (window 2) were selected and simulated in the TRNSYS model through the same time period of the experiment and the comparative results are shown in Fig. 5 and Fig. 6 accordingly.

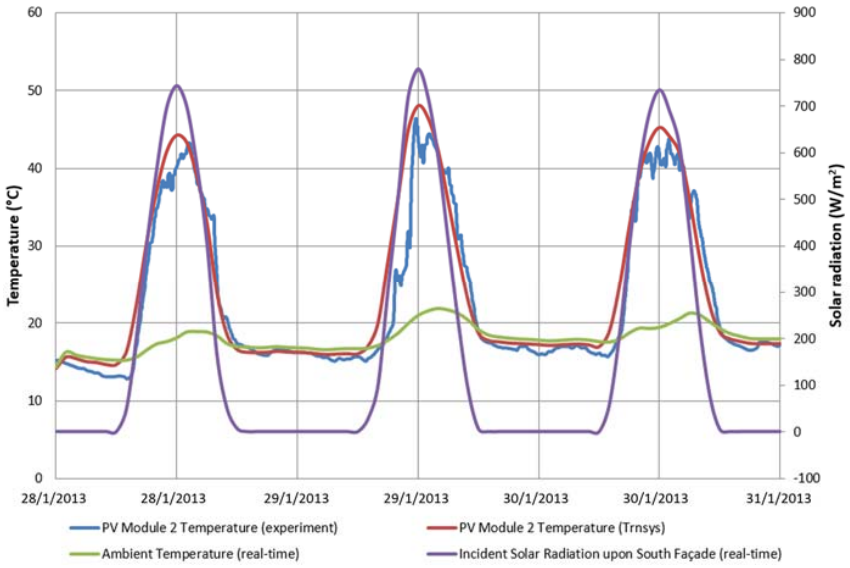

Fig. 5: PV module temperature comparison in Mode 2 (buoyancy ventilation).

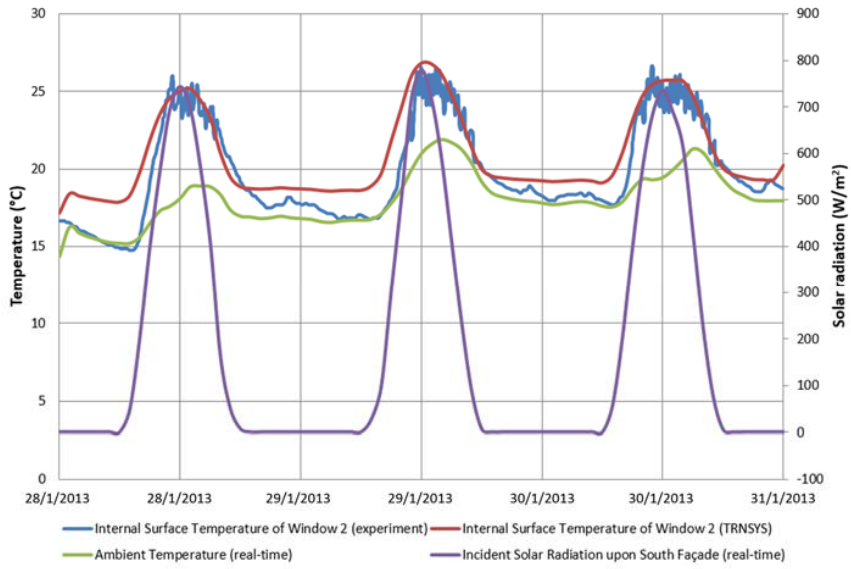

Fig. 6: Comparisons for internal surface temperature of Window 2 in Mode 2 (buoyancy ventilation).

As shown in Fig. 5, the hourly values of PV module temperature show acceptable agreement with the

experimental results and the corresponding hourly MBE and CVRMSE were -4.85% and 11.6% respectively. Comparison of the simulated and measured hourly internal surface temperature of window 2 shows obvious differences during the troughs, in which the simulated values are consistently exceeding the measured values and the biggest difference reached about 3°C in Fig. 6. A likely explanation is the different thermal behaviors between the used window glazing in TRNSYS and the experiment as the experimental information of the window was not available (Peng, Lu, & Yang, 2013), a float glass was assigned to window 2 in the TRNSYS model. In addition, it is difficult to model natural ventilation directly in TRNSYS. This could be done by coupling with the external plug-in such as TRNFlow and CONTAM, but it is outside the scope of this stage of study. As an alternative, the buoyancy-driven ventilation in the cavity was modelled in terms of the constant mass flow rate as the window speeds during the 72 hours were basically floating at 2m/s according to the real-time weather data, so the simulated curve (internal surface temperature of window 2) was much steadier than the curve of measured values. Moreover, the related MBE and CVRMSE were -5.51% and 7.28% respectively, which were acceptable and hence the TRNSYS model for mode 2 was deemed validated.

4. Preliminary Numerical Simulation Model for the BIPV/T-DSF in Australia

In terms of the validated TRNSYS model, a preliminary numerical simulation model has been developed for investigating the thermal performance of the novel BIPV/T-DSF system and its impact on indoor thermal comfort of a commercial building in Sydney, Australia. A building model was built in TRNSYS which was based on the experimental test bed but facing due north in Sydney. The building fabric, except for the PV glazing of the simulation model was modified in the generic design for a better evaluation of the indoor thermal response by use of the BIPV/T-DSF. In order to understand the performance of the BIPV/T-DSF system, the indoor air temperature under the typical days in summer and winter were analyzed accordingly.

4.1. Fan-Driven Ventilated Operation in Summer

A fan-driven ventilating operation for the model building in Sydney was modelled in TRNSYS using a constant mass flow rate (1.35 kg/hour from the validated model in section 3.2) for a steady state of analysis for 72 hours' simulation. In this operation mode, there was no air-conditioning in the building model, the inlet and outlet louvers on the both cavities were opened to allow buoyancy ventilation, which was then compared to the building model operated without the BIPV/T-DSF system. In order to eliminate other uncertainties which might interfere the simulation results, the internal gains from people, equipment and lightings were not included in the models.

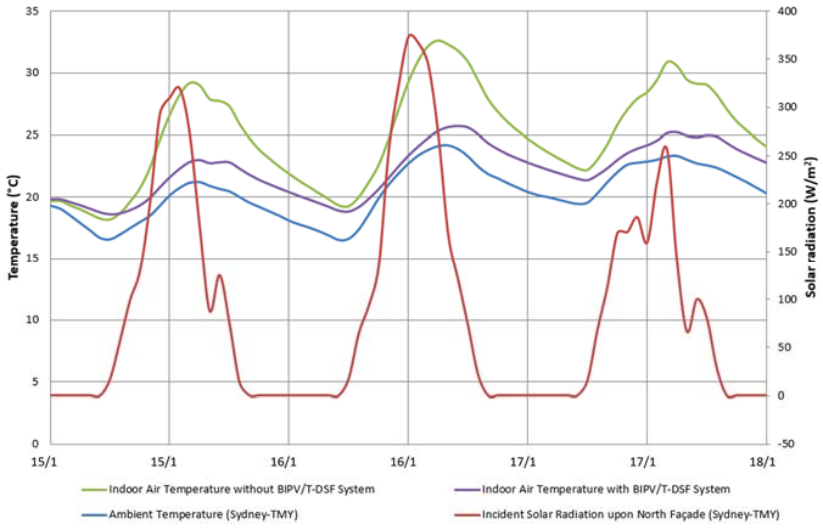

Fig. 7: Comparisons for indoor air temperature with/without BIPV/T-DSF system in summer.

Fig. 7 presents the indoor air temperatures with/without the application of BIPV/T-DSF system for the building model from Jan 15 to Jan 18 in the typical summer days in Sydney. It was found that the indoor air temperature of the building either with or without the BIPV/T-DSF system was always higher than the ambient temperature

throughout the day. The main reason is that the accumulations of solar heat gain led to a higher indoor air temperature than ambient temperature. However, the building model that utilized the BIPV/T-DSF system has significantly lower indoor air temperature than the building model without a BIPV/T-DSF and reached a maximum temperature of 6°C lower during the daytime. This indicated the BIPV/T-DSF system can reduce the indoor air temperature and assist in reduce the thermal load on the mechanical cooling system.

4.2. Non-Ventilated Operation in Winter

Based on the results in section 4.1, all the louvers and windows of the BIPV/T-DSF system were closed for winter to avoid the heat loss through the ventilation. The comparisons between the building adopting and not adopting the non-ventilated BIPV/T-DSF system were compared from Aug 15 to Aug 18 for typical winter days in Fig. 8. It can be seen that the indoor air temperature of the building model either with or without BIPV/T-DSF system was always higher than the ambient temperature, and the indoor air temperature can be maintained at a comfort level during the daytime. Clearly, the temperature drops at night time due to the heat loss through the building fabric, while the BIPV/T-DSF system brought the thermal buffer benefit that played a passive heating role in winter, but the ventilated operation of the cavity can be used for the higher solar radiation days (i.e. Aug 15 and Aug 17) to maintain a lower and comfort indoor air temperature. The non-BIPV/T-DSF case has an overheating issue during the peak daytime and the highest indoor temperature reached about 42°C on Aug 15.

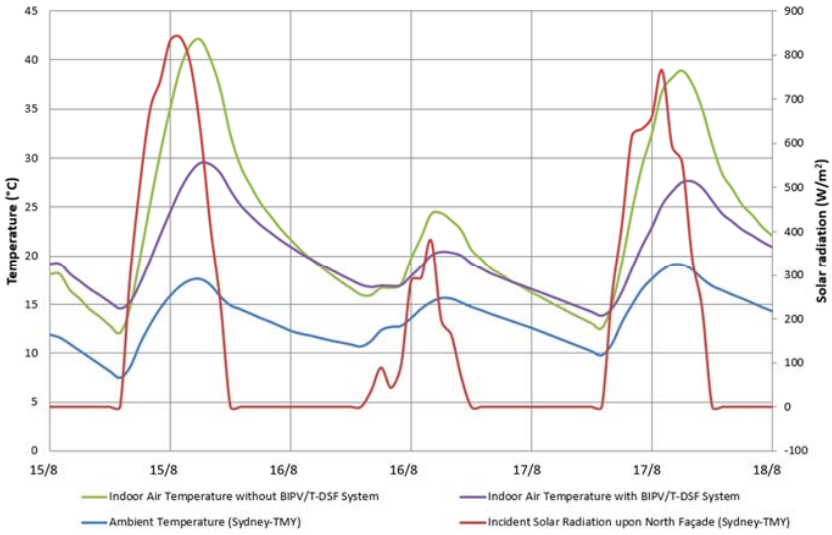

Fig. 8: Comparisons for indoor air temperature with/without BIPV/T-DSF system in winter.

5. Conclusions

The simulation results show that BIPV/T-DSF system gives not only good thermal performance in terms of buffering the building from summer heat gains, but reduces heat loss as well as overheat of building during winter time in the subtropical climate areas in southern hemisphere like Sydney. These are preliminary studies of the novel building façade technology that remains provisional since they are parts of the ongoing research. Further studies will concentrate on developing the specific strategies for maximizing its thermal and electrical performance, and optimizing the long term indoor thermal comfort using the strategies.

Acknowledgements

The authors would like to acknowledge the financial support provided by the Faculty of Built Environment, University of New South Wales (Australia) and the Cooperative Research Centre for Low Carbon Living (CRC-LCL). The authors also would like to express the deepest gratitude to Dr. Jinqing Peng for providing the indispensable input data of the test bed.

References

ASHRAE. (2002). Guideline 14-2002 *Measurement of Energy and Demand Savings*. Atlanta, Georgia: American Society of Heating, Ventilating, and Air Conditioning Engineers.

Athienitis, A. K., Bambara, J., O'Neill, B., & Faille, J. (2011). A prototype photovoltaic/thermal system integrated with transpired collector. *Solar Energy, 85*(1), 139-153. doi:10.1016/j.solener.2010.10.008

Bazilian, M., Kamalanathan, H., & Prasad, D. (2002). Thermographic analysis of a building integrated photovoltaic system. *Renewable Energy, 26*(3), 449-461.

Bazilian, M. D., Leenders, F., Ree, B. G. C. V. d., & Prasad, D. (2001). Photovoltaic cogeneration in the built environment. *Solar Energy, 71*(1), 57-69.

Charron, R., & Athienitis, A. K. (2006). Optimization of the performance of double-façades with integrated photovoltaic panels and motorized blinds. *Solar Energy, 80*(5), 482-491. doi:10.1016/j.solener.2005.05.004

Chen, Y., Athienitis, A. K., & Galal, K. (2010). Modeling, design and thermal performance of a BIPV/T system thermally coupled with a ventilated concrete slab in a low energy solar house: Part 1, BIPV/T system and house energy concept. *Solar Energy, 84*(11), 1892-1907. doi:10.1016/j.solener.2010.06.013

Chikate, B. V., & Sadawarte, Y. A. (2015). *The Factors Affecting the Performance of Solar Cell*. Paper presented at the International Journal of Computer Applications (0975-8887), Maharashtra, India.

Chow, T. T., Hand, J. W., & Strachan, P. A. (2003). Building-integrated photovoltaic and thermal applications in a subtropical hotel building. *Applied Thermal Engineering, 23*(16), 2035-2049. doi:10.1016/s1359-4311(03)00183-2

Chwieduk, D. A. (2017). Towards modern options of energy conservation in buildings. *Renewable Energy, 101*, 1194-1202. doi:10.1016/j.renene.2016.09.061

Council of Australian Governments. (2012). *Baseline Energy Consumption and Greenhouse Gas Emissions in Commercial Buildings in Australia (Part 1)*. Canberra: Department of Climate Change and Energy Efficiency.

Fossa, M., Ménézo, C., & Leonardi, E. (2008). Experimental natural convection on vertical surfaces for building integrated photovoltaic (BIPV) applications. *Experimental Thermal and Fluid Science, 32*(4), 980-990. doi:10.1016/j.expthermflusci.2007.11.004

Ghaffarianhoseini, A., Ghaffarianhoseini, A., Berardi, U., Tookey, J., Li, D. H. W., & Kariminia, S. (2016). Exploring the advantages and challenges of double-skin façades (DSFs). *Renewable and Sustainable Energy Reviews, 60*, 1052-1065. doi:10.1016/j.rser.2016.01.130

Kamel, R. S., & Fung, A. S. (2014). Modeling, simulation and feasibility analysis of residential BIPV/T+ASHP system in cold climate—Canada. *Energy and Buildings, 82*, 758-770. doi:10.1016/j.enbuild.2014.07.081

Marques da Silva, F., Gomes, M. G., & Rodrigues, A. M. (2015). Measuring and estimating airflow in naturally ventilated double skin facades. *Building and Environment, 87*, 292-301. doi:10.1016/j.buildenv.2015.02.005

Mekhilef, S., Saidur, R., & Safari, A. (2011). A review on solar energy use in industries. *Renewable and Sustainable Energy Reviews, 15*(4), 1777-1790. doi:10.1016/j.rser.2010.12.018

Oliver, M., & Jackson, T. (2000). The evolution of economic and environmental cost for crystalline silicon photovoltaics. *Energy Policy, 28*(14), 1011-1021.

Pantic, S., Candanedo, L., & Athienitis, A. K. (2010). Modeling of energy performance of a house with three configurations of building-integrated photovoltaic/thermal systems. *Energy and Buildings, 42*(10), 1779-1789. doi:10.1016/j.enbuild.2010.05.014

Papaefthimiou, S., Syrrakou, E., & Yianoulis, P. (2006). Energy performance assessment of an electrochromic window. *Thin Solid Films, 502*(1-2), 257-264. doi:10.1016/j.tsf.2005.07.294

Peng, J., Curcija, D. C., Lu, L., Selkowitz, S. E., Yang, H., & Zhang, W. (2016). Numerical investigation of the energy saving potential of a semi-transparent photovoltaic double-skin facade in a cool-summer Mediterranean climate. *Applied Energy, 165*, 345-356. doi:10.1016/j.apenergy.2015.12.074

Peng, J., Lu, L., & Yang, H. (2013). An experimental study of the thermal performance of a novel photovoltaic double-skin facade in Hong Kong. *Solar Energy, 97*, 293-304. doi:10.1016/j.solener.2013.08.031

Peng, J., Lu, L., Yang, H., & Han, J. (2013). Investigation on the annual thermal performance of a photovoltaic wall mounted on a multi-layer façade. *Applied Energy, 112*, 646-656. doi:10.1016/j.apenergy.2012.12.026

Peng, J., Lu, L., Yang, H., & Ma, T. (2015). Comparative study of the thermal and power performances of a semi-transparent photovoltaic façade under different ventilation modes. *Applied Energy, 138*, 572-583. doi:10.1016/j.apenergy.2014.10.003

Peng, J., Lu, L., Yang, H., Song, A., & Ma, T. (2015, 25 to 27 August). *182: Investigation on the overall energy performance of an a-si based photovoltaic double-skin facade in Hong Kong.* Paper presented at the Proceedings of the 14th International Conference on Sustainable Energy Technologies, Nottingham, UK.

Raftery, P., Keane, M., & Costa, A. (2011). Calibrating whole building energy models: Detailed case study using hourly measured data. *Energy and Buildings, 43*(12), 3666-3679. doi:10.1016/j.enbuild.2011.09.039

Saadon, S., Gaillard, L., Giroux-Julien, S., & Ménézo, C. (2016). Simulation study of a naturally-ventilated building integrated photovoltaic/thermal (BIPV/T) envelope. *Renewable Energy, 87*, 517-531. doi:10.1016/j.renene.2015.10.016

United Nations Environment Programme. (2016). Sustainable Buildings and Climate Initiative: Promoting Policies and Practies for Sustainability. Retrieved from http://www.unep.org/sbci/AboutSBCI/Background.asp

Vats, K., Tomar, V., & Tiwari, G. N. (2012). Effect of packing factor on the performance of a building integrated semitransparent photovoltaic thermal (BISPVT) system with air duct. *Energy and Buildings, 53*, 159-165. doi:10.1016/j.enbuild.2012.07.004

Yang, T., & Athienitis, A. K. (2012). *Investigation of performance enhancement of a building integrated photovoltaic thermal system.* Paper presented at the Proceedings of the Canadian Conference on Building Simulation, Halifax, Canada.

Yang, T., & Athienitis, A. K. (2015). Experimental investigation of a two-inlet air-based building integrated photovoltaic/thermal (BIPV/T) system. *Applied Energy, 159*, 70-79. doi:10.1016/j.apenergy.2015.08.048